Horizon detection based on sky-color and edge features

Article *in* Proceedings of SPIE - The International Society for Optical Engineering · January 2008

DOI: 10.1117/12.766689

CITATIONS
19

READS
600

2 authors:

Bahman Zafarifar
Technische Universiteit Eindhoven
15 PUBLICATIONS **104** CITATIONS
SEE PROFILE

Hans Weda
Philips
43 PUBLICATIONS **334** CITATIONS
SEE PROFILE

Horizon detection based on sky-color and edge features

Bahman Zafarifar[1] and Hans Weda[2] and Peter H. N. de With[3]

[1]NXP Research, High Tech Campus 32, room 140, 5656AE Eindhoven, The Netherlands
[2]Philips Research, High Tech Campus 34, room 4049, 5656 AE Eindhoven, The Netherlands
[3]Eindhoven Univ. of Technology, P.O. Box 513, 5600 MB, Eindhoven, The Netherlands

ABSTRACT

Horizon detection in still images or video sequences contributes to applications like image understanding, automatic correction of image tilt and image quality enhancement. In this paper, we propose an algorithm for detecting the horizon line in digital images, which employs an edge-based and a new color-based horizon detection technique. The color-based detector calculates an estimate of the horizon line by analyzing the color transition in the clear sky areas of the image. The edge-based detector computes the horizon line by finding the most prominent line or edge in the image, based on Canny edge detection and Hough transformation. The proposed algorithm combines the two detectors into a hybrid detection system, thereby taking advantage of their complimentary strengths. We have applied the algorithm on a manually annotated set of images and evaluated the accuracy of the position and angle of the detected horizon line. The experiments indicate the usefulness of the proposed color-based detector (40% lower error vs. the edge-based detector) and the benefit of the adopted approach for combining the two individual detectors (57% and 17% lower error vs. the edge-based and the color-based detectors, respectively).

Keywords: horizon detection, video content analysis, sky detection, image understanding

1. INTRODUCTION

Human perception of visual information is influenced by the composition of objects in the visual content. Basic compositional elements are described by mathematics and include lines, forms, masses and movement.[1] Lines constitute an important element in interpretation and understanding of the content. In still images and video sequences, the horizon line is of particular interest because it forms a natural line that separates the sky from the rest of the image, and as such influences human interpretation of the context. Hence, automatic horizon detection contributes to understanding the scene content, and may enable applications at various levels, as exemplified below.

At semantic level, horizon detection enables applications like indoor/outdoor classification and image context understanding. This type of information is valuable for content-based image categorization and content-based search and retrieval of image and video material from databases. A practical example of using horizon detection at semantic level is the application in high-end TV systems. Here, the knowledge about the existence and angle of the horizon can support automatic understanding of the scene atmosphere (line and scene orientation influences human perception as indicated in psycho-visual literature[1]). The television may respond to this information, e.g. by adapting the audiovisual scheme to match indoor/outdoor scenes. Another conceivable application in high-end TVs is the augmentation of the recent background lighting technology (in which the TV projects spatiotemporally dynamic colors on the background wall), to incorporate the semantic-level information derived from horizon detection.

At image level, horizon detection line can be used for automatic or assisted re-alignment of tilted images (Fig. 1), or for stitching multiple photos into one panoramic image. A different application of horizon detection at scene level is autonomous robotic systems and vision-based automatic control systems for aviation.[2]

Lastly, horizon detection can facilitate pixel-level applications by accurate segmentation of sky areas in an image. Examples are content-adaptive image enhancement of sky areas, or contribution to depth estimation in 2D-to-3D conversion applications. In the latter, the knowledge of the horizon line may be used for assigning appropriate depth values to sky and ground areas.

Visual Communications and Image Processing 2008, edited by William A. Pearlman, John W. Woods, Ligang Lu,
Proc. of SPIE-IS&T Electronic Imaging, SPIE Vol. 6822, 682220, © 2008 SPIE-IS&T · 0277-786X/08/$18

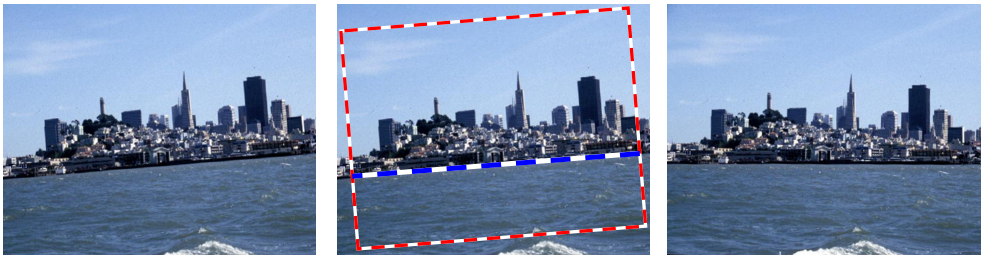

Figure 1. Correction of a tilted image using horizon detection. (a) input image, (b) detected horizon line, (c) corrected image tilt.

Horizon detection literature includes methods based on edge detection.[3,4] The basic principle of such methods is computing the horizon line by detecting the most prominent edge in the image, using edge detection on the image followed by Hough transformation. Images that contain prominent straight edges other than the horizon line, may therefore form a problem for such edge-based techniques.

Cornall and Egan[5] propose a simple color-based method for horizon detection, where image pixels are classified to sky/ground classes, and the angle of the horizon line is estimated to be perpendicular to the line connecting the centers of the sky and the center of the ground areas. Here, the sky/ground classification is based on the assumption that sky is brighter and bluer than ground, and is implemented by thresholding the blue signal component. It is understandable that using such simple approach, bright or blue objects in the ground plane, or a significant color change of sky along the zenith-to-horizon direction could lead to detection errors.

We propose a horizon detection system that exploits the physical phenomenon of color de-saturation and brightness increase along the zenith-to-horizon direction in clear sky areas,[6,7] in order to calculate a first estimate of the position and the angle of the horizon. This color-based detector first classifies clear sky regions using color, texture, gradient and position features, and subsequently estimates the horizon position through analyzing the mentioned chromatic change in clear sky areas. These estimates are then refined by an edge-based detection technique, which employs Canny edge detection and Hough transform. The color-based detector uses only the color of clear sky areas and is not influenced by edges and structures in other parts of the image. The edge-based detector can precisely determine the position and the angle of a clearly visible horizon line, and is independent of sky areas. Consequently, the two detectors have complementary strengths.

The aim of our experiment is to demonstrate the usefulness of the proposed color-based detection technique, especially when this is combined with an alternative horizon detection technique (edge-based in our case). Our evaluation on a manually annotated test set shows that the proposed combination outperforms the individual detectors in the accuracy of the computed horizon position and angle.

In the remainder of this paper, Sec. 2 describes the algorithm, Sec. 3 presents the experimental results and Sec. 4 is devoted to the conclusions.

2. DESCRIPTION OF THE HYBRID ALGORITHM

In the following subsections, we describe the edge-based and the color-based detectors, followed by the description of the combination approach.

2.1 Edge-based horizon detection

The horizon line separates the sky areas from the rest of the image. The difference in image properties on the two sides of the horizon line, such as color and texture properties, causes that the horizon often forms a prominent edge in the image. Therefore, the edge-based detector aims at detecting the principal edge in the image. The detector first computes a binary edge map and subsequently identifies the most prominent straight line in this edge map.

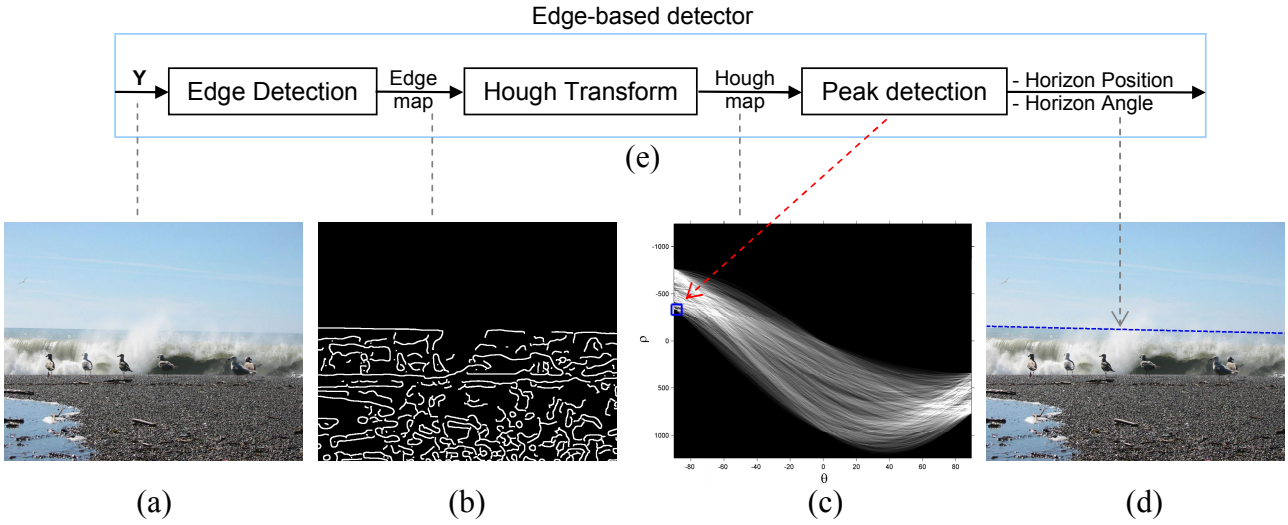

Figure 2. Edge-base horizon detection. (a) input image, (b) result of the Canny edge detector, (c) Hough map, (d) horizon detection result, (e) schematic overview.

Figure 2 depicts the edge-based horizon detector. In the first step, Canny edge detection[8] is performed on the luminance component of the image. Since we are only interested in the most prominent straight edges, we choose a large variance (σ) for the low-pass filter of the Canny edge detector. This smoothes the detailed edges and concentrates on the main structures of the image. This yields a binary image (edge map) that contains the significant edges (Fig. 2(b)).

The next step aims at identifying straight lines in the edge map. For this purpose, we apply the Hough transform[9] to the edge map. The Hough transform is a means of detecting straight lines in the image. It transforms the edge map from the spatial domain to the Hough space. The Hough transform uses the parametric representation of a line, described by

$$\rho = x \cdot \cos(\theta) + y \cdot \sin(\theta), \tag{1}$$

where x and y are coordinates in the spatial domain, and θ and ρ are the coordinates in the Hough space. Considering a line in the spatial domain, ρ stands for the distance from the image origin (top-left corner of the image) to this line along a vector perpendicular to the line, and θ is the angle between the horizontal axis and this vector.

The Hough map, shown in Fig. 2(c), can be seen as an intensity map, in which coordinates with high values (bright positions) represent straight lines in the image (in our case the edge map). Therefore, the most prominent straight line in the edge map can be found by identifying the point in the Hough map that has the highest value (indicated by the small square at the left side of Fig. 2(c)). The result is shown in Fig. 2(d).

The edge-based detector has the following characteristics.

- It is accurate in calculating the horizon position and the angle when a clear horizon line is present, and when other straight edges are less dominant than the horizon line. In this case, the accuracy of the detection is only limited by the resolution of the Hough map.
- It is accurate in calculating the horizon angle when lines parallel to the horizon exist. Images usually contain a plurality of edges parallel to the horizon line. Using appropriate filtering in the Hough space, these parallel edges could be combined in order to detect the angle of the horizon.
- It is mislead by non-horizon straight edges (Fig. 6(a, b)). The edge-based detector cannot distinguish between the edge corresponding to the actual horizon line and other prominent straight edges.
- It fails when no clear horizon line exist in the image (Fig. 6(c)). For example, this occurs when the horizon is occluded by objects, such as mountains, trees or buildings.

2.2 Color-based horizon detection

We mentioned above that the edge-based detector generates erroneous results in case no clear horizon line exists in the image, or in case other prominent straight edges than the horizon line occur. This susceptibility could be reduced if the system incorporates a detection technique that is not affected by edges in the image. This motivates the use of the color-based horizon detector.

Clear sky is often characterized by shade of saturated blue at the top of the image, while gradually desaturating to almost white toward the horizon line. This phenomenon is caused primarily by the larger thickness of air masses between our eyes and the horizon, compared to the zenith.[6,7,10]

We have observed that the above-mentioned sky color phenomenon is translated to an increase in the luminance, and a decrease in the chrominance in the vertical direction towards the horizon (along the direction of zenith to horizon). Based on this property, we can calculate an estimate of the horizon line, i.e. the vertical position of the horizon and its angle, by analyzing the color of the clear sky areas. For this purpose, we first classify the image to (clear) sky/non-sky classes. The horizon position is then computed by analyzing the change of the average color values in the vertical direction of the image (1D analysis), while the horizon angle is calculated by analyzing the change of the color values of the sky pixels in the 2D space. This is further elaborated below (see also Fig. 3).

The first step for color-based horizon detection is calculating a continuous sky probability map, P_{sky} in Fig. 3(e), representing the probability of each pixel belonging to clear sky. Clear sky areas have the following properties: (1) they are more likely to be located in the upper part of the image, (2) they have a certain range of color, when limited to day-light condition, (3) they contain low texture, (4) the speed of change in color values in the horizontal and the vertical directions (gradient in luminance and chrominance components) is limited, and (5) there is often a luminance increase and chrominance decrease along the zenith-to-horizon direction. Based on these considerations, we compute the sky probability P_{sky} using color, position, texture, and gradient features, by the expression

$$P_{sky} = P_{position} \cdot P_{color} \cdot P_{texture} \cdot P_{gradient} \quad . \tag{2}$$

Here, the vertical-position feature $P_{position}$ introduces a higher probability for pixels located higher in the image. The color feature P_{color} is implemented by a 3D Gaussian function in the YUV color space. The texture feature $P_{texture}$ removes textured areas, using the Sum of Absolute Differences between the luminance values of neighboring pixels. The gradient feature $P_{gradient}$ removes areas that have excessive spatial gradients in the luminance component. The gradient feature also exploits the aforementioned knowledge about the chromatic change in the vertical direction for rejecting areas that do not fit to the expected range of luminance increase and chrominance decrease in the vertical direction towards the horizon. This helps eliminating objects that have a color similar to sky, such as the reflection of sky in water or other sky-colored objects. For a better rejection of non-sky objects, the texture and the gradient features are performed on multiple scales (resolutions) of the image, after which the results are combined together. The reader is referred to[11,12] for more details.

The second step for color-based horizon detection is segmenting the sky pixels by converting the continuous sky probability map to a binary map (sky mask in Fig. 3(f)), using an adaptive threshold value which is based on the histogram of the sky probability.[11] This binary map classifies each pixels to either sky or non-sky class.

The third step is computing the horizon position. This is based on the previously mentioned observation on the luminance increase and chrominance decrease along the zenith-to-horizon direction, and the often occurring discontinuity in the color values above and below the horizon line. We first compute the average the pixel color values in the horizontal direction over the pixels labeled as sky. This yields a one-dimensional estimate of the sky color in the vertical direction (Fig. 3(g)). Next, using this 1D average (vertical) color, we compute the horizon position as the point at which (1) the luminance increases to a maximum, (2) the chrominance decreases to a minimum, and (3) a discontinuity in the values occurs. Additionally, we calculate a confidence measure that indicates the reliability of the computed horizon position, based on the amount of changes in the luminance and chrominance, and the strength of the mentioned discontinuity. This confidence metric defines to what extent the result of the color-based horizon detection influences the final horizon detection.

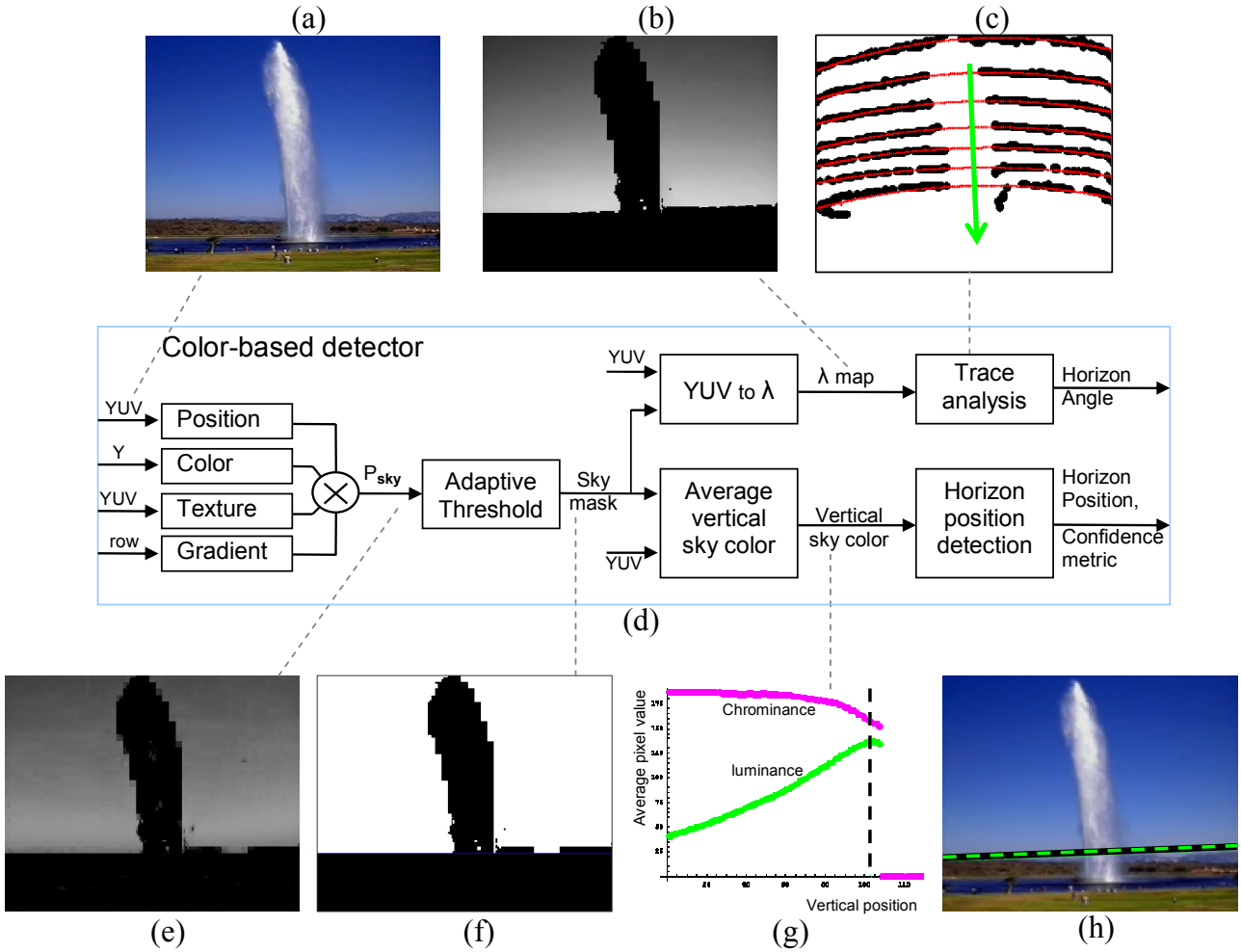

Figure 3. Color-based detection. (a) input image, (b) map of λ, (c) map of λ sliced between a series of increasing threshold values. Bold traces indicate pixels having similar λ vales, while thin traces indicate 2^{nd} degree polynomials connecting the pixels of each trace. The arrow indicates the direction of maximum ascent of λ (perpendicular to the horizon line), (d) schematic overview, (e) sky probability map, (f) segmented sky pixels (binary sky mask), (g) average color values of sky pixels in the vertical direction. The upper trace is the chrominance (combined U and V), while the lower trace is the luminance. The dashed vertical line on the right side indicates the horizon position, (h) detected horizon line in the image.

The forth step for color-based horizon detection involves the computation of the horizon angle. This is again based on the mentioned luminance increase and chrominance decrease along the zenith-to-horizon direction. The objective is to determine the direction in which the above-mentioned chromatic change is steepest. We first reduce the dimensionality by combining the YUV color components to a single component λ, using a linear combination given by

$$\lambda = c_y \cdot Y + c_u \cdot U + c_v \cdot V \quad . \tag{3}$$

Here, coefficients c_y, c_u and c_v are chosen such that the mentioned chromatic change along the zenith-to-horizon direction in each color component (Y, U and V), results to an increase of λ.

Figure 3(b) shows the 2D map of λ corresponding to the input image. The chromatic change along the zenith-to-horizon direction is represented in this image by the increasing intensity of the pixels as we move from the zenith towards the horizon. This 2D map of λ is then analyzed over the pixels labeled as sky, for determining the direction in which the gradient is steepest. For this purpose, we slice (threshold) the 2D map of λ between

a series of increasing threshold levels, in order to produce traces (series of pixels) of similar λ values. These traces are shown in Figure 3(c) by bold dots. Finally, a 2^{nd} degree polynomial is fitted to each trace and the average direction of the polynomials is taken as an estimate of the horizon angle. The fitted functions are shown in Fig. 3(c)) by the thin dots.

The color-based horizon detector has the following characteristics.

- It does not require a clear horizon line to be visible in the image. In other words, horizon lines occluded by objects do not form a problem for this detector (Fig. 6(c)).
- It is not mislead by straight lines in the image (Fig. 6(a, b)).
- The calculated horizon position and angle are not accurate (Fig. 4(c)).
- Wrong detection may result when the sun or thin clouds influence the sky color, or when large objects with image properties similar to sky exist in the image (Fig. 6(d)).

2.3 Combining the color-based and the edge-based detectors

As described previously, each of the two approaches has its advantages and drawbacks. Mainly, the edge-base detector is susceptible to straight edges or occlusion of the horizon line, and the color-based detector is inaccurate

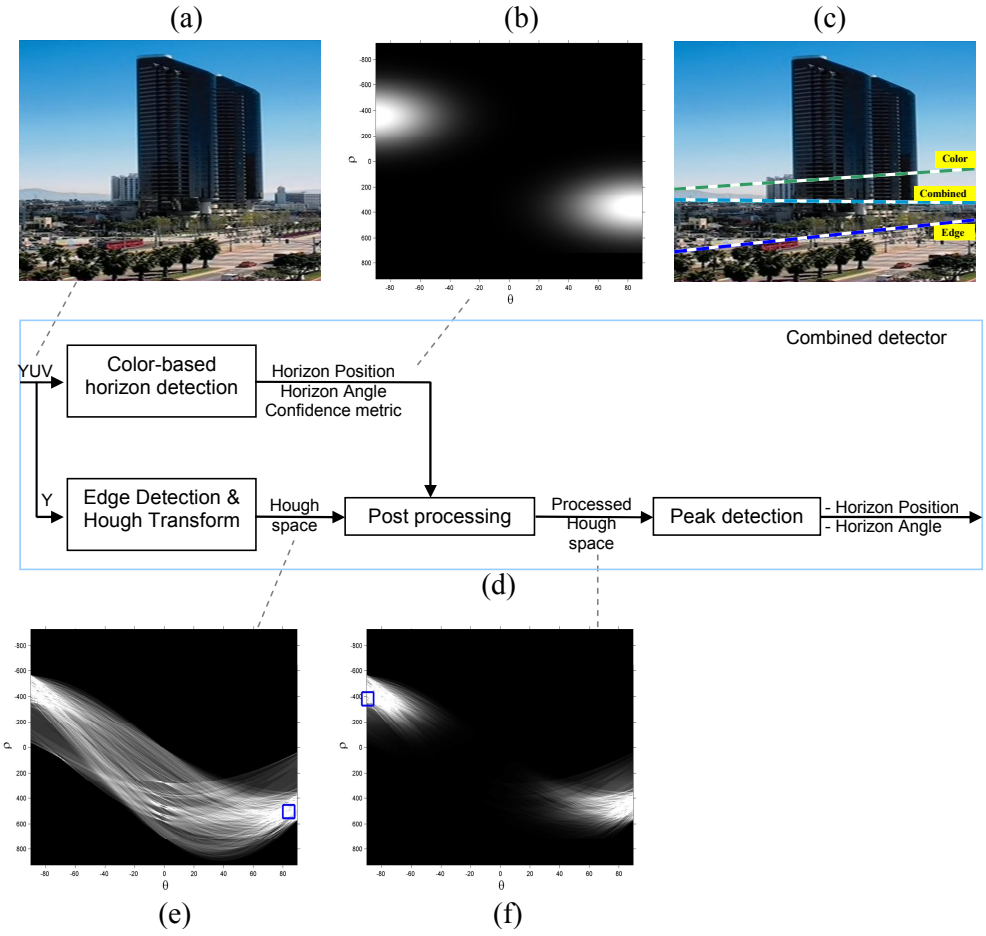

Figure 4. Processing steps in the combined detector. (a) input image, (b) weighting factor for post-processing, centered at Hough space representation of the horizon position and angle obtained from the color-based detector, (c) detection result, (d) schematic overview, (e) Hough transform of the detected edges, (f) Hough transform multiplied by the weighting factor.

and is influenced by sky-colored objects or deviations in the color of the sky. We propose a combination of the two detectors that results in a system that is more robust than each of the detectors individually.

Figure 4 depicts the combined system in which the parameters calculated by the color-based detector (horizon position, angle and confidence metric) are used to post-process the result of the Hough transform, prior to identifying the point with the highest value in the Hough map, as a final output. More specifically, we first create a weighting factor in the form of a 2D Gaussian function in the Hough space, of which the center coordinates are defined by the horizon angle and position obtained from the color-based detector (Fig. 4(b)). The confidence metric further determines the amplitude and offset of this 2D Gaussian weighting function. Next, we multiply this weighting function with the result of the Hough transform from the edge-based detector (Fig. 4(e)). This produces the post-processed Hough map in Fig. 4(f). The horizon line is now found by identifying the point in this post-processed Hough map that has the highest value.

The combined detector compensates the lack of detection accuracy of the color-based detector with the high precision of the edge-based detector. Likewise, the susceptibility of the edge-based detector to non-horizon straight lines, or failure in the absence of a clear horizon line, is alleviated by the incorporated initial estimates provided by color-based detector.

3. EXPERIMENTAL RESULTS

The proposed combined algorithm and the two individual detectors were applied on a test set of 100 images, including images with clear horizon line, images with obstructed horizon and images containing prominent straight edges. The result was evaluated by comparing the position and the angle of the detected horizon line with the manually-annotated horizon line. The results are shown in Table 1. The *absolute error* indicates the absolute difference between each parameter (*position* and *angle*) and the corresponding parameter of the manually-annotated horizon line. The *relative error* is the *absolute error* normalized to the corresponding parameter of the *edge-based* detector.

Figure 5 visualizes the relative error in a bar diagram. In this figure,we notice that the average *absolute error* (mean of horizon position and angle error) of the combined detector is 57% lower the edge-based detector (43% vs. 100%), and 17% lower than the color-based detector (vs. 43% vs. 60%). In other words, the combined algorithm performs clearly better than the individual detectors, both in the position and the angle of the horizon line. The results also suggest that the color-based detector performs better than the edge-based detector by 40% (60% vs. 100%) on our test set. This can be explained by the observation that images typically contain straight lines forming structures and objects in the image, which can be falsely detected as the horizon line by the edge-based detector. In addition, the frequent occlusions of the horizon line by objects, such as mountains or buildings, impede a good performance of the edge-based detector. The adopted color-based horizon detection can deal with these problems, as it is merely based on the sky color.

Figure 6 presents a few examples of the individual and the combined detection results. Figure 6(a, b) illustrate situations where the edge-based detector wrongly identifies straight edges as horizon, whereas the combined algorithm is able to detect the horizon correctly, due to the color-based algorithm. Figure 6(c) shows that the absence of a clear horizon line does not form a problem for the color-based detector. Finally, in Fig. 6(d) both detectors, and also the combined algorithm fail. Here, the color-based algorithm fails due to the close color similarity between the sky and the sea, while the edge-based detector fails due to the blurred sky-to-sea transition and the sharp coast line.

4. CONCLUSIONS

We have presented an new algorithm for detecting horizon lines in digital images. The main aim is to demonstrate that it is possible to use the chromatic changes in clear sky areas for detecting the horizon line, without relying on other parts of the image, and that such a detector can assist other horizon detection methods. The proposed algorithm employs an edge-based and a new color-based horizon detector and thereby exploits the individual strengths of both detectors. The color-based detector determines the position and the angle of the horizon line by analyzing the characteristic color transition of clear sky areas along the zenith-to-horizon direction. This allows the system to determine the horizon even in images where the actual horizon line is occluded, albeit with

Table 1. Detection results of the combined algorithm vs. the individual horizon detectors on 100 images. *Absolute error* indicates the absolute difference between each parameter (*position* and *angle*) and the corresponding parameter of the manually-annotated horizon line. *Relative error* is the *absolute error* normalized to the corresponding parameter of the *edge-based* detector.

Method	***Edge-based***		***Color-based***		***Combined***	
Feature	***Position*** *(pixels)*	***Tilt*** *(degrees)*	***Position*** *(pixels)*	***Tilt*** *(degrees)*	***Position*** *(pixels)*	***Tilt*** *(degrees)*
Absolute Error *(with respect to manually defined horizon)*	80.46	10.56	45.89	6.66	42.62	3.44
Relative Error *(with respect to manually defined horizon, normalized to edge-based method)*	100%	100%	57%	63%	53%	33%

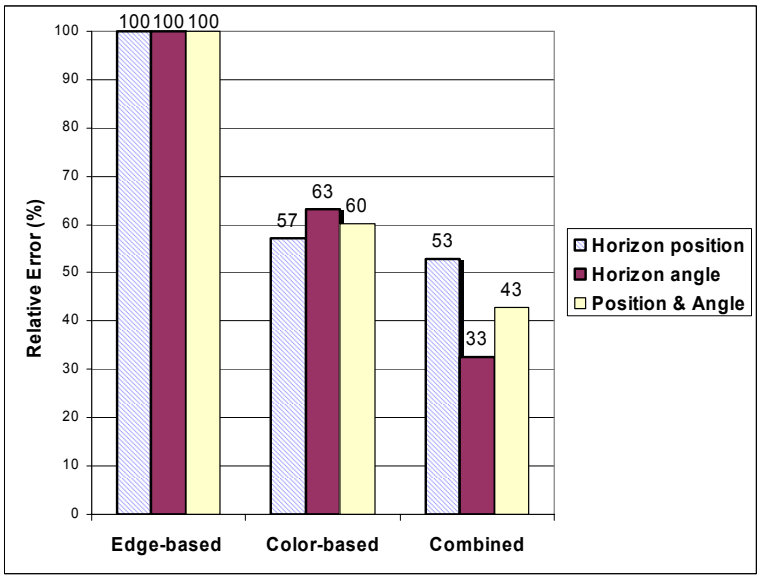

Figure 5. Relative error of the individual detectors and the combined algorithm (normalized to the edge-based detector). The combined algorithm performs significantly better than the individual detectors in both the position and the angle of the horizon, for the test set.

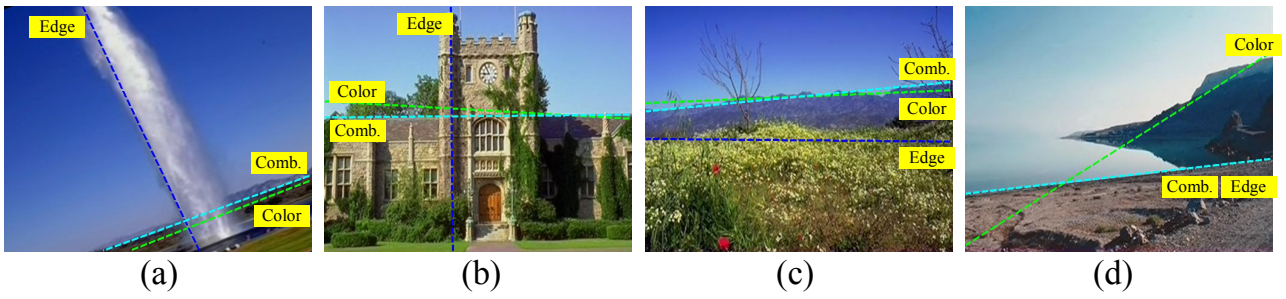

Figure 6. Examples of individual and combined detection results. The output of the edge-based, the color-based and the combined algorithm are indicated by *Edge*, *Color* and *Comb.*, respectively.

a lower accuracy. Our experiments prove the usefulness of the proposed color-based detector (40% lower average error than the edge-based detector) and the benefit of the adopted approach for combining the two individual detectors; the combined detection algorithm alleviates the average detection error with 57% and 17%, when compared to the edge-based and the color-based detectors, respectively.

The presented work has not been optimized for detection accuracy, robustness and computational load, and is therefore not benchmarked against existing algorithms. We expect that the edge-based detector can be improved by applying a filter on the Hough space for favoring horizontal lines over tilted or vertical lines, or a filter for combining parallel straight lines in the image. With respect to complexity, we estimate that the curve-fitting stage in the color-based detector is computationally expensive and not suited for embedded applications. Therefore, further optimization of this stage is desirable for embedded applications.

5. ACKNOWLEDGMENTS

The authors would like to thank Philips Innovative Applications (Bruges, Belgium) for financial support of the project, and Mauro Barbieri and Dragan Sekulovski from Philips Research for useful discussions.

REFERENCES

1. J. V. Mascelli, *"The Five C's of Cinematography"*, Silman-James Press, 1998.
2. S. Todorovic and M. Nechyba, "A vision system for intelligent mission profiles of micro air vehicles," in *IEEE Transactions on Vehicular Technology*, *6* **53**, pp. 1713–1725, November 2004.
3. G. Bao, Z. Zhou, S. Xiong, X. Lin, and X. Ye, "Towards micro air vehicle flight autonomy research on the method of horizon extraction," in *Instrumentation and Measurement Technology Conference, 2003. IMTC '03. Proceedings of the 20th IEEE*, **2**, pp. 1387–1390, May 2003.
4. D. Dusha, W. Boles, and R. Walker, "Fixed-wing attitude estimation using computer vision based horizon detection," in *Proceedings of 12th Australian International Aerospace Congress*, pp. 1–19, March 2007.
5. T. Cornall and G. Egan, "Measuring horizon angle from video on a small unmanned air vehicle," in *The 2nd International Conference on Autonomous Robots and Agents (ICARA)*, pp. 339–344, December 2004.
6. C. F. Bohren and D. R. Huffman, *"Absorption and Scattering of Light by Small Particles"*, Wiley-Interscience, 1998.
7. D. K. Lynch and W. Livingston, *"Color and Light in Nature"*, Cambridge University Press, 2001.
8. J. Canny, "A computational approach to edge detection," in *IEEE Trans. Pattern Analysis and Machine Intelligence*, *8*, pp. 679–714, November 1986.
9. R. Gonzalez and R. Woods, *"Digital Image Processing"*, Prentice Hall, 1993.
10. J. Luo and S. P. Etz, "A physical model-based approach to detecting sky in photographic images," *IEEE Transactions on Image Processing* **11**(3), pp. 201–212, 2002.
11. B. Zafarifar and P. H. N. de With, "Adaptive modeling of sky for video processing and coding applications," in *27th Symposium on Information Theory in the Benelux*, pp. 31–38, June 2006.
12. B. Zafarifar and P. H. N. de With, "Blue sky detection for picture quality enhancement," in *Advanced Concepts for Intelligent Vision Systems (Acivs)*, pp. 522–532, September 2006.